NASA/TM—2015-218815

A Radiation Solver for the National Combustion Code

Peter M. Sockol
Glenn Research Center, Cleveland, Ohio

July 2015

NASA STI Program . . . in Profile

Since its founding, NASA has been dedicated to the advancement of aeronautics and space science. The NASA Scientific and Technical Information (STI) Program plays a key part in helping NASA maintain this important role.

The NASA STI Program operates under the auspices of the Agency Chief Information Officer. It collects, organizes, provides for archiving, and disseminates NASA's STI. The NASA STI Program provides access to the NASA Technical Report Server—Registered (NTRS Reg) and NASA Technical Report Server—Public (NTRS) thus providing one of the largest collections of aeronautical and space science STI in the world. Results are published in both non-NASA channels and by NASA in the NASA STI Report Series, which includes the following report types:

- TECHNICAL PUBLICATION. Reports of completed research or a major significant phase of research that present the results of NASA programs and include extensive data or theoretical analysis. Includes compilations of significant scientific and technical data and information deemed to be of continuing reference value. NASA counter-part of peer-reviewed formal professional papers, but has less stringent limitations on manuscript length and extent of graphic presentations.

- TECHNICAL MEMORANDUM. Scientific and technical findings that are preliminary or of specialized interest, e.g., "quick-release" reports, working papers, and bibliographies that contain minimal annotation. Does not contain extensive analysis.

- CONTRACTOR REPORT. Scientific and technical findings by NASA-sponsored contractors and grantees.

- CONFERENCE PUBLICATION. Collected papers from scientific and technical conferences, symposia, seminars, or other meetings sponsored or co-sponsored by NASA.

- SPECIAL PUBLICATION. Scientific, technical, or historical information from NASA programs, projects, and missions, often concerned with subjects having substantial public interest.

- TECHNICAL TRANSLATION. English-language translations of foreign scientific and technical material pertinent to NASA's mission.

For more information about the NASA STI program, see the following:

- Access the NASA STI program home page at http://www.sti.nasa.gov

- E-mail your question to help@sti.nasa.gov

- Fax your question to the NASA STI Information Desk at 757-864-6500

- Telephone the NASA STI Information Desk at 757-864-9658

- Write to:
  NASA STI Program
  Mail Stop 148
  NASA Langley Research Center
  Hampton, VA 23681-2199

NASA/TM—2015-218815

A Radiation Solver for the National Combustion Code

Peter M. Sockol
Glenn Research Center, Cleveland, Ohio

National Aeronautics and
Space Administration

Glenn Research Center
Cleveland, Ohio 44135

July 2015

Level of Review: This material has been technically reviewed by technical management.

Available from

NASA STI Program
Mail Stop 148
NASA Langley Research Center
Hampton, VA 23681-2199

National Technical Information Service
5285 Port Royal Road
Springfield, VA 22161
703-605-6000

This report is available in electronic form at http://www.sti.nasa.gov/ and http://ntrs.nasa.gov/

A Radiation Solver for the National Combustion Code

Peter M. Sockol
National Aeronautics and Space Administration
Glenn Research Center
Cleveland, Ohio 44135

Abstract

A methodology is given that converts an existing finite volume radiative transfer method that requires input of local absorption coefficients to one that can treat a mixture of combustion gases and compute the coefficients on the fly from the local mixture properties. The Full-spectrum *k*-distribution method is used to transform the radiative transfer equation (RTE) to an alternate wave number variable, g. The coefficients in the transformed equation are calculated at discrete temperatures and participating species mole fractions that span the values of the problem for each value of g. These results are stored in a table and interpolation is used to find the coefficients at every cell in the field. Finally, the transformed RTE is solved for each g and Gaussian quadrature is used to find the radiant heat flux throughout the field. The present implementation is in an existing cartesian/cylindrical grid radiative transfer code and the local mixture properties are given by a solution of the National Combustion Code (NCC) on the same grid. Based on this work the intention is to apply this method to an existing unstructured grid radiation code which can then be coupled directly to NCC.

Introduction

The National Combustion Code (NCC) is a state of the art Computational Fluid Dynamics (CFD) program specifically designed for combustion processes (Ref. 1). The code employs an unstructured grid, massively parallel computing (Refs. 2 and 3), a dynamic wall function with the effect of adverse pressure gradient (Ref. 4), a low Reynolds number wall treatment (Ref. 5), a cubic non-linear *k*-epsilon turbulence model (Ref. 6), a lagrangian liquid phase spray model (Ref. 7), and stiff laminar chemistry integration. Recently, viscous low-speed preconditioning (Ref. 8) has been added to improve the low-speed convergence of the NCC in viscous regions and the ability to handle multiple sets of periodic boundary conditions has also been added. The combination of these features is usually not available in other CFD codes and gives the NCC an advantage when computing recirculating, turbulent, reacting spray flows. Previously, the NCC has undergone extensive validation studies for simple flows (Ref. 9), complex flows (Ref. 10), NO_x emissions prediction (Ref. 11) and traditional gas turbine combustor injectors (Ref. 12).

For most high-temperature combustion problems, thermal radiation plays an important role in the heat transfer to the surrounding surfaces and the absorption and emission of radiation can also have a significant effect on the temperature distribution throughout the domain. Hence, if a designer wanted to use NCC to aid in the design of a jet engine combustor or a furnace combustion chamber, it would be very useful to be able to compute the radiative transfer as part of the process. In this work we have taken a significant step in that direction.

At present two codes exist for solving the radiative transfer equation (RTE). The first is a stand-alone cartesian or cylindrical grid code (Ref. 13) that solves in 1D, 2D, or 3D. The second is an unstructured grid code (Ref. 14) that could be coupled with NCC. Both of these codes require input of the local absorption coefficients. Hence the user of either code needs a means of coming up with at least approximate values of the absorption coefficients as a function of gas properties and wave number.

A gas emits and absorbs radiation only at wave numbers in the vicinity of spectral lines. Since the main participating gases (CO_2 and H_2O) each have more than one million absorption/emission lines, it would be impractical to solve the RTE at enough wave numbers to resolve this physics. Modest and coworkers have developed a methodology for handling this behavior by transforming the RTE to an

alternate wave number variable space where the coefficients vary smoothly (Ref. 15). We currently have a Spectral Radiation Calculation Software package (Ref. 16) (SRCS) which includes source code and data sets necessary to run the method as part of another application.

In this work we use the existing cartesian/cylindrical radiation code modified to solve in the transformed wave number space. We also use the Modest full-spectrum *k*-distribution method and adapt the SRCS package to run with the modified cartesian/cylindrical radiation code. NCC is run on a cartesian grid to obtain local temperatures and species mole fractions. SRCS is used to obtain a table of absorption coefficients at discrete values of temperature and participating species mole fractions where these properties span the range of values from the NCC solution. We next interpolate within the table to obtain cell center values of *k* for every cell in the grid. Finally, we run the modified cartesian/cylindrical radiation code with these *k* values to obtain radiation intensity and heat transfer throughout the field. The expectation is that this same methodology will work quite well with the unstructured grid radiation code and thus provide a solver that can be coupled with NCC.

Full-Spectrum *k*-Distribution Method

Over the years Modest and coworkers have added significant refinements to the basic method (Refs. 17 to 21). These increase the accuracy for inhomogeneous gas mixtures, but they also increase the complexity of the method. Since the turbulence-chemistry modeling used in NCC is still undergoing significant development, it was decided to use the basic full-spectrum *k*-distribution (FSK) method in this work (Ref. 15). In addition, since radiation scattering is not considered important for combustion gases, this effect is neglected (Ref. 22). Also, while the presence of soot affects emission and absorption, scattering by soot is typically negligible.

We begin with the spectral radiative transfer equation for an absorbing/emitting medium:

$$\frac{dI_\eta}{ds} = \kappa_\eta\left(\underline{\phi},\eta\right)\left[I_{b\eta}(T) - I_\eta\right], \tag{1}$$

where I_η is the spectral intensity varying along a path s, η is the wavenumber, κ_η is the spectral absorption coefficient, $I_{b\eta}$ is the Planck function and $\underline{\phi} = \left(T, p, \underline{x}\right)$ is an array of state variables. Here $\underline{x}$ is the mole fraction vector. We reorder the absorption coefficient in Equation (1) by multiplying by the delta function $\delta\left(k - \kappa_\eta\left(\eta, \underline{\phi}_0\right)\right)$, and integrating over the entire spectrum. Here $\kappa_\eta\left(\eta, \underline{\phi}_0\right)$ is the absorption coefficient evaluated at some reference state $\underline{\phi}_0 = \left(T_0, p_0, x_0\right)$. This gives

$$\frac{dI_k}{ds} = k^*\left(\underline{\phi},k\right)\left[f\left(T,\underline{\phi}_0,k\right)I_b(T) - I_k\right], \tag{2}$$

provided that at every wavenumber across the spectrum where $\kappa_\eta\left(\underline{\phi}_0,\eta\right)$ has one and the same value k, we also have a unique value for $\kappa_\eta\left(\underline{\phi},\eta\right) = k^*\left(\underline{\phi},k\right)$. In Equation (2) I_k and f are defined as

$$I_k = \int_0^\infty I_\eta \delta\left(k - \kappa_\eta\left(\underline{\phi}_0,\eta\right)\right) d\eta, \tag{3}$$

$$f\left(T,\underline{\phi}_0,k\right) = \frac{1}{I_b}\int_0^\infty I_{b\eta}(T)\delta\left(k - \kappa_\eta\left(\underline{\phi}_0,\eta\right)\right) d\eta. \tag{4}$$

In terms of the cumulative *k*-distribution,

$$g\left(T,\underline{\phi}_0,k\right)=\int_0^k f\left(T,\underline{\phi}_0,k\right)dk=\int_0^{k^*} f\left(T,\underline{\phi},k^*\right)dk^*=g\left(T,\underline{\phi},k^*\right), \tag{5}$$

the RTE becomes:

$$\frac{dI_g}{ds}=k^*\left(T_0,\underline{\phi},g\right)\left[a(T,T_0,g)I_b(T)-I_g\right], \tag{6}$$

where

$$I_g=I_k/f\left(T_0,\underline{\phi}_0,k\right), \tag{7}$$

$$a(T,T_0,g)=f\left(T,\underline{\phi}_0,k\right)/f\left(T_0,\underline{\phi}_0,k\right), \tag{8}$$

and $k^*\left(T_0,\underline{\phi},g\right)$ is the k vs. g distribution as given by Equation (5), with the absorption coefficient evaluated at the local conditions $\underline{\phi}$ and the Planck function evaluated at the reference temperature T_0.

The reordered spectral intensity I_g can be obtained by solving the modified RTE, Equation (6), and the spectrally integrated intensity is then evaluated as

$$I=\int_0^\infty I_\eta d\eta=\int_0^\infty \mathrm{I}_k f\left(T_0,\underline{\phi}_0,k\right)dk=\int_0^1 I_g dg. \tag{9}$$

Since I_g is a smooth function of g, the integral in Equation (9) can be evaluated by Gaussian quadrature with values of I_g computed and stored at the quadrature points. Similarly the integrated heat flux in any direction can also be found by Gaussian quadrature.

Use of the SRCS package

The SRCS package (Ref. 16) can be used to calculate the k versus g distribution as a function of the local state variables $\underline{\phi}$. However, to do this at every cell in a large 3D computation would be prohibitively expensive. Instead we construct a multidimensional table using discrete values of temperature and participating species mole fractions that span the values from the NCC solution. The SRCS software is used to populate the table with values of k_q versus g_q where the g_q are the Gaussian quadrature points. We then interpolate within the table to obtain cell center values of k_q for each g_q at every spatial cell in the field. Note the same process is used to obtain a_q for each g_q at every cell.

We begin by calculating the reference state $\underline{\phi_0}$. Following Modest (Ref. 15) we choose a volume averaged mole-fraction and a Planck-mean temperature:

$$\underline{x_0}=\frac{1}{V}\int_V \underline{x}\,dV, \tag{10}$$

$$\kappa_P\left(T_0, \underline{x_0}\right) = \frac{1}{V}\int_V \kappa_P\left(T, \underline{x}\right) I_b(T) dV, \tag{11}$$

and it is assumed that the pressure variation across the domain is negligible. For combustor simulations, the volume V for these averages would be restricted to regions with significant concentrations of combustion products (i.e., regions downstream of fuel injectors).

Next, for each $\left(T, \underline{x}\right)$ grouping, we obtain the $k\left(T_0, \underline{\phi}, g\right)$ distribution using the SRCS software, interpolate within the distribution to obtain k_q for each g_q and store the k_q in the table. Also, for each T in the table, we obtain $a(T, T_0, g)$, interpolate to get a_q for each g_q and store the a_q in a second table. Since the absorption coefficients are expected to be more sensitive to T than to $\underline{x}$, for the first table we construct cubic spline fits for k_q versus T for each $\underline{x}$ and g_q. We also construct cubic spline fits for a_q versus T for each g_q.

Once this preliminary work has been completed, we proceed to compute k_q and a_q for each cell in the field by interpolating within the two tables. Since for the present work we consider only two participating species (CO_2 and H_2O), the spline fit is used to find k_q for the local T at the four corners of a box containing the local $\underline{x}$. Bilinear interpolation is then used to find the local value of k_q. For three or four participating species this is readily extended to trilinear or quadralinear interpolation. We use the spline fit in the second table to find a_q at the local T.

Solution of the Radiative Transfer Equation

The cartesian/cylindrical solver used in this study (Ref. 13) uses a finite volume method to solve the transformed RTE, Equation (6). First note that I_g depends on both the spatial coordinates and the radiation direction (polar angle θ and azimuthal angle ϕ). We integrate Equation (6) over a control volume ΔV and a control angle $\Delta\Omega$ and apply the divergence theorem to obtain

$$\int_{\Delta\Omega}\int_{\Delta A} I_g(\hat{\boldsymbol{s}}\cdot\hat{\boldsymbol{n}}) dA d\Omega = \int_{\Delta\Omega}\int_{\Delta V} k^*\left(T_0, \underline{\phi}, g\right)\left[a(T, T_0, g) I_b(T) - I_g\right] dV d\Omega \tag{12}$$

where $\hat{\boldsymbol{s}}$ is the unit vector in the radiation direction and $\hat{\boldsymbol{n}}$ is the outward unit normal along the control surface ΔA. If the intensity is assumed constant over the control volume ΔV_i, then Equation (12) can be rewritten as

$$\sum_j I_{ij}^l D_{ij}^l \Delta A_{ij} = -B_i^l I_i^l + S_i^l, \tag{13}$$

where the summation is over the faces of ΔV_i, I_{ij}^l is the intensity at face ΔA_{ij} of ΔV_i in direction $\hat{\boldsymbol{s}}^l$,

$$D_{ij}^l = \int_{\Delta\Omega^l}\left(\hat{s}\cdot\hat{n}_{ij}\right) d\Omega \tag{14}$$

$$B_i^l = k_i^* \Delta V_i \Delta\Omega^l, \tag{15}$$

$$S_i^l = k_i^* a_i (I_b)_i \Delta V_i \Delta\Omega^l, \tag{16}$$

and the subscript *g* has been dropped to simplify the notation. The face intensities I_{ij}^{l} are obtained from the step scheme. For $D_{ij}^{l} > 0$ (an outflow of radiant energy), we use I_{i}^{l} the center value of ΔV_i . For $D_{ij}^{l} < 0$ (an inflow of radiant energy) we use $I_{i'}^{l}$ the center value of the adjacent control volume $\Delta V_{i'}$ except where ΔA_{ij} lies on a domain boundary and a boundary condition is used to obtain I_{ij}^{l}. Finally, the directional space is defined by taking constant spacing for θ and ϕ, where θ is measured relative to $\hat{e}_z$ and ϕ is measured relative to $\hat{e}_x$ in the $\hat{e}_x - \hat{e}_y$ plane.

For a cartesian grid the solution of Equation (13) is straightforward. Start at one of the eight corners of the 3D domain and select that octant of the total directional space for which all the directions point into the interior of the grid. For each of these directions we sweep through the grid in such a way that all of the radiant inflow to a control volume comes either from adjacent control volumes that have been updated during the current sweep or from the adjacent boundary condition. Next move to another corner and repeat the process for a different octant of the directional space. After all eight corners have been used, the radiation intensity I_{i}^{l} will have been updated for every control volume ΔV_i and control angle $\Delta\Omega^{l}$ in the entire domain.

Sample Cases

Hot Gas Cylinder

Before we present results from a combustion problem, we consider a simple case to show the kinds of results that can be obtained from the current cartesian/cylindrical radiation code. We choose a cylinder of hot gas with cold walls. The gas temperature T_g is set to 1000 K, the pressure P_g to 1 atm. and the mole fractions x_{pg} of the participating gases to 0.2 and 0.02 for CO_2 and H_2O, respectively. The walls are set to 0 K. Symmetry conditions are used to reduce the domain to radial distance $r = 0$ to *rmax* and axial distance $z = 0$ to 4 *rmax* with symmetry at $r = 0$ and $z = 0$. Even though the problem is axisymmetric, the azimuthal distance goes from $\varphi = 0$ to 2π. The number of spatial grid cells is taken as $20\varphi \times 40r \times 100z$ with hyperbolic tangent stretching used to cluster the cells near the walls in *r* and *z*. The grid spacing in φ is kept uniform. The directional discretization uses $8\theta \times 20\phi$ with uniform spacing in both directions. Finally we note that we solve the RTE for each of 10 Gaussian quadrature points g_q. The final distributions of $q_r\,, q_z\,, G\ and\ div(q)$ are then found by Gaussian quadrature.

For a first calculation we set *rmax* = 1.0 m. The resulting distributions are shown in Figure 1, where each of the variables is divided by an appropriate reference value: $qref = \sigma T_g^4, Gref = qref/\pi,\ dvref = qref/rmax$ and σ is the Stefan-Boltzman constant. In Figure 1(a) the radial heat flux rises gradually from zero at the centerline to a maximum at $r = rmax$, in Figure 1(b) the axial heat flux is close to zero until the end wall is approached at $z = 4$ *rmax*, in Fig. 1(c) the mean radiative intensity is largest at the centerline and decreases gradually as the cold walls are approached and finally in Figure 1(d) the radiative heat source is negligible until very near the cold walls. Thus this is an optically thick case.

As a second calculation we set *rmax* = 0.01 m. The resulting distributions are shown in Figure 2, where the reference values are the same as in Figure 1 except that $dvref$ is 100 times as large. The results shown in Figure 2(a) to (c) are similar to those in Figure 1. However, Figure 2(d) shows that the radiative heat source, while negligible near most of the centerline, gradually becomes substantial as the cold walls are approached. Thus this case could be considered optically thin.

Sandia Flame D (Ref. 23)

This is one of a series of piloted CH_4/air flames that were set up to provide data to test combustion models. In this case a mixture of 25% CH_4 and 75% dry air enters at a temperature of 294 K and mean velocity of 49.6 m/sec through the main jet located on the centerline with a diameter $d = 7.2$ mm. The jet

exit Reynolds number is 22400. The annular pilot, which surrounds the jet, has an outer diameter of 18.2 mm. Burnt gas from the pilot enters at a mean temperature of 1880 K and a mean velocity of 11.4 m/sec. Outside the pilot, dry air enters at a temperature of 291 K and a mean velocity of 0.9 m/sec. The entering composition of the pilot gas and the velocity and turbulence profiles, which were measured separately (Ref. 24), are given in the above reference.

This flame was simulated with NCC on a domain with radial distance r = 0 to 0.045 m and axial distance z = 0 to 0.375 m. A 2D-axisymmetric grid is used with 120 cells in r clustered at the outer edge of the jet, and 100 cells in z gradually stretching from the inlet to the exit. Axisymmetric flow was assumed. The calculations used a k-epsilon turbulence model with only linear terms retained in the Reynolds stress. The chemistry model used finite rate chemistry with 12 species and 10 reactions and no turbulence-chemistry interaction. The resulting distributions are shown in Figure 3. Figure 3(a) shows hot temperatures reaching the centerline very close to the jet exit in contrast to the experimental data (Ref. 23) where large temperatures along the centerline occur at $z/d > 15$. Figure 3(b) and (c) show that CO_2 and H_2O mass fractions also reach large values on the centerline very close to the jet exit. The poor prediction for the flame location is likely a result of the lack of turbulence-chemistry interaction in these calculations. Since the purpose of this work is to demonstrate the capability of the radiation solver with input from NCC, this combustion simulation is still relevant.

For the cartesian/cylindrical radiation solver, r and z are taken from the NCC grid and, although the problem is axisymmetric, the azimuthal distance φ again goes from $\varphi = 0$ to 2π. The radiation solver spatial grid is taken as $20\varphi \times 120r \times 100z$ and the directional grid is taken as $8\theta \times 20\phi$ control angles. The local transformed absorption coefficents k^* are calculated from the local values of temperature and mole fractions of the two participating species (CO_2 and H_2O) as obtained from the NCC solution. As in the above case we again solve the RTE for each of 10 Gaussian quadrature points and obtain the final distributions of $q_r\,, q_z\,, G\ and\ div(q)$ by Gaussian quadrature. The resulting distributions are shown in Figure 4. Note the reference values are as defined for the Hot Gas Cylinder above with T_g set to 2000 K and *rmax* replaced by the jet diameter d = 0.0072 m. Since there are no solid walls, the temperatures on the domain boundaries are taken from the values at the adjacent grid cell and the emissivity on these boundaries is taken as 1.0. As a result Figure 4(a) and (b) shows that the radial and axial heat fluxes are relatively uninteresting. Figure 4(c) shows the radiant intensity increasing with z as the temperature increases. Figure 4(d) shows the radiative heat source largest in the interior of the flame along the centerline.

Finally it should be noted that for this case the computer cost for the two codes is comparable. In particular, on an HP Z400 workstation, the time per iteration per cell was 1.8×10^{-4} sec for NCC while for the cartesian/cylindrical radiation code this time was 1.5×10^{-4} sec per spatial cell for a single solution of the RTE. Since in general it takes far fewer iterations to converge the RTE than it does for NCC, it would be quite practical to couple the two codes by running the radiation code every 10 to 100 iterations of NCC and then updating the radiation source term in the energy equation of NCC. This would allow the temperature distribution to adjust to the presence of the radiation coming from the flame.

Concluding Remarks

This paper presents a methodology for converting an existing finite volume radiative heat transfer method with input absorption coefficients to one that can treat a mixture of combustion gases and compute the coefficients on the fly from the local mixture properties. The Full- spectrum k-distribution method is used to transform the radiative transfer equation (RTE) to an alternate wave number variable, g. A Spectral Radiation Calculation Software package is used to calculate the transformed absorption coefficients at discrete values of temperatures and participating species mole fractions that span the values of the problem for each value of g. These results are stored in a table and interpolation is used to obtain cell centered values of the coefficients for every cell in the field. Finally, the transformed RTE is solved

for each g and Gaussian quadrature is used to find the radiant heat transfer, mean radiant intensity and radiant heat source throughout the field.

In the present work the methodology is implemented in an existing cartesian/cylindrical grid radiation code and local mixture properties are obtained from a solution of the NCC on the same grid. The method is readily extendable to unstructured grids and provides the foundation for coupling radiation heat transfer with the flow solver in NCC.

References

1. Stubbs, R.M. and Liu, N.-S., (1997), "Preview of the National Combustion Code," AIAA-97-3114, 33rd AIAA/ASME/SAE/ASEE Joint Propulsion Conference & Exhibit, July 6-9, Seattle, WA, USA.
2. Quealy, A., Ryder, R., Norris, A. and Liu, N.-S., (2000), "National Combustion Code: Parallel Implementation and Performance," NASA/TM—2000-209801.
3. Quealy, A., (2002), "National Combustion Code Parallel Performance Enhancements," NASA/CR—2002-211340.
4. Shih, T.-H., Povinelli, L.A. and Liu N.-S., (2003), "Application of Generalized Wall Function for Complex Turbulent Flows," Journal of Turbulence, Vol. 4, No. 15, pp 1-16.
5. Chien, K.Y., (1982), "Prediction of Boundary Layer Flows with a Low-Reynolds-Number Turbulence Model," AIAA J., Vol. 20, No.1, pp 33-38.
6. Shih, T.-H., Chen, K.-H. and Liu, N.-S., (1998), "A Non-Linear k-epsilon Model for Turbulent Shear Flows," AIAA-98-3983, 34th AIAA/ASME/SAE/ASEE Joint Propulsion Conference & Exhibit, July 13-15, Cleveland, OH, USA.
7. Raju, M.S., (2004), "LSPRAY-II: A Lagrangian Spray Module," NASA/CR—2004-212958.
8. Choi, Y.-H. and Merkle, C. L., (1993), "The Application of Preconditioning in Viscous Flows," J. Comput. Phys., Vol. 105, pp 207-223.
9. Chen, K.-H., Norris, A.T., Quealy, A. and Liu, N.-S., (1998), "Benchmark Test Cases for The National Combustion Code," AIAA-98-3855, 34th AIAA/ASME/SAE/ASEE Joint Propulsion Conference & Exhibit, July 13-15, Cleveland, OH, USA.
10. Iannetti, A., Tacina, R., Jeng, S.-M. and Cai, J., (2001), "Towards Accurate Prediction of Turbulent, Three-Dimensional, Recirculating Flows with the NCC," NASA/TM—2001-210761, AIAA-2001-0809.
11. Shih, T.-H., Norris, A., Iannetti, A.C., Marek, C.J., Smith, T.D., Liu, N.-S. and Povinelli, L.A., (2001), "A Study of Hydrogen/Air Combustor Using NCC," AIAA-2001-808, 39th Aerospace Sciences Meeting & Exhibit, Jan. 8-11, Reno, NV, USA.
12. Iannetti, A.C. and Chen, K.-H., (2000), "An Initial Comparison of National Combustion Code Simulations Using Various Chemistry Modules with Experimental Gas Turbine Combustor Data," AIAA-2000-0330, 38th Aerospace Sciences Meeting, Reno, NV, USA.
13. Chai, J.C., Lee, H.S. and Patankar, S.V., (1994), "Finite Volume Method for Radiation Heat Transfer," Journal of Thermophysics and Heat Transfer, Vol. 8, No. 3, pp 419-425.
14. Moder, J.P., Kumar, G.N. and Chai, J.C., (2000), "An Unstructured-Grid Radiative Heat Transfer Module for the National Combustion Code," AIAA 2000-0453, 38th Aerospace Sciences Meeting, Reno, NV, USA.
15. Modest, M.F., (2003), "Narrow-Band and Full-Spectrum k-Distributions for Radiative Heat Transfer – Correlated-k vs. Scaling Approximation," Journal of Quantitative Spectroscopy & Radiative Transfer, Vol. 76, pp 69-83.
16. Modest, M.F., (2008), "Spectral Radiation Calculation Software," copyrighted package provided by the copywriter, Michael F. Modest.
17. Modest, M.F. and Riazzi, R.J., (2005), "Assembly of Full-Spectrum k-Distributions from a Narrow-Band Database; Effects of Mixing Gases, Gases and Nongray Absorbing Particles, and Mixtures with Nongray Scatterers in Nongray Enclosures," Journal of Quantitative Spectroscopy & Radiative Transfer, Vol. 90, pp 169-189.

18. Wang, L. and Modest, M.F., (2005), "Narrow-Band Based Multiscale Full-Spectrum *k*-Distribution Method for Radiative Transfer in Inhomogeneous Gas Mixtures," Journal of Heat Transfer, Vol. 127, pp 740-748.
19. Pal, G., Modest, M.F. and Wang, L., (2008), "Hybrid Full-Spectrum Correlated *k*-Distribution Method for Radiative Transfer in Nonhomogeneous Gas Mixtures," Journal of Heat Transfer, Vol. 130, pp 082701-082708.
20. Pal, G. and Modest, M.F., (2009), "A Multiscale Full-Spectrum *k*-Distribution Method for Radiative Transfer in Nonhomogeneous Gas-Soot Mixtures with Wall Emission," An International Journal of Computational Thermal Sciences, Vol. 1, pp 1-22.
21. Pal, G. and Modest, M. F., (2010), "A Narrow Band-Based Multiscale Multigroup Full-Spectrum *k*-Distribution Method for Radiative Transfer in Nonhomogeneous Gas-Soot Mixtures," Journal of Heat Transfer, Vol. 132, pp 0233071-0233079.
22. Viskanta, R. and Menguc, M.P., (1987), "Radiation Heat Transfer in Combustion Systems," Prog. Energy Combust. Sci., Vol. 13, pp 97-160.
23. Barlow, R. and Frank, J., (2007), "Piloted CH_4/Air Flames C, D, E, and F – Release 2.1," www.sandia.gov/TNF/DataArch/FlameD/SandiaPilotDoc21.pdf.
24. Schneider, Ch., Dreizler, A., Janicka, J. and Hassel, E. P., (2003), "Flow Fie-ld Measurements of Stable and Locally Extinguishing Hydrocarben-Fuelled Jet Flames," Combustion and Flame, Vol. 135, pp 185-190.

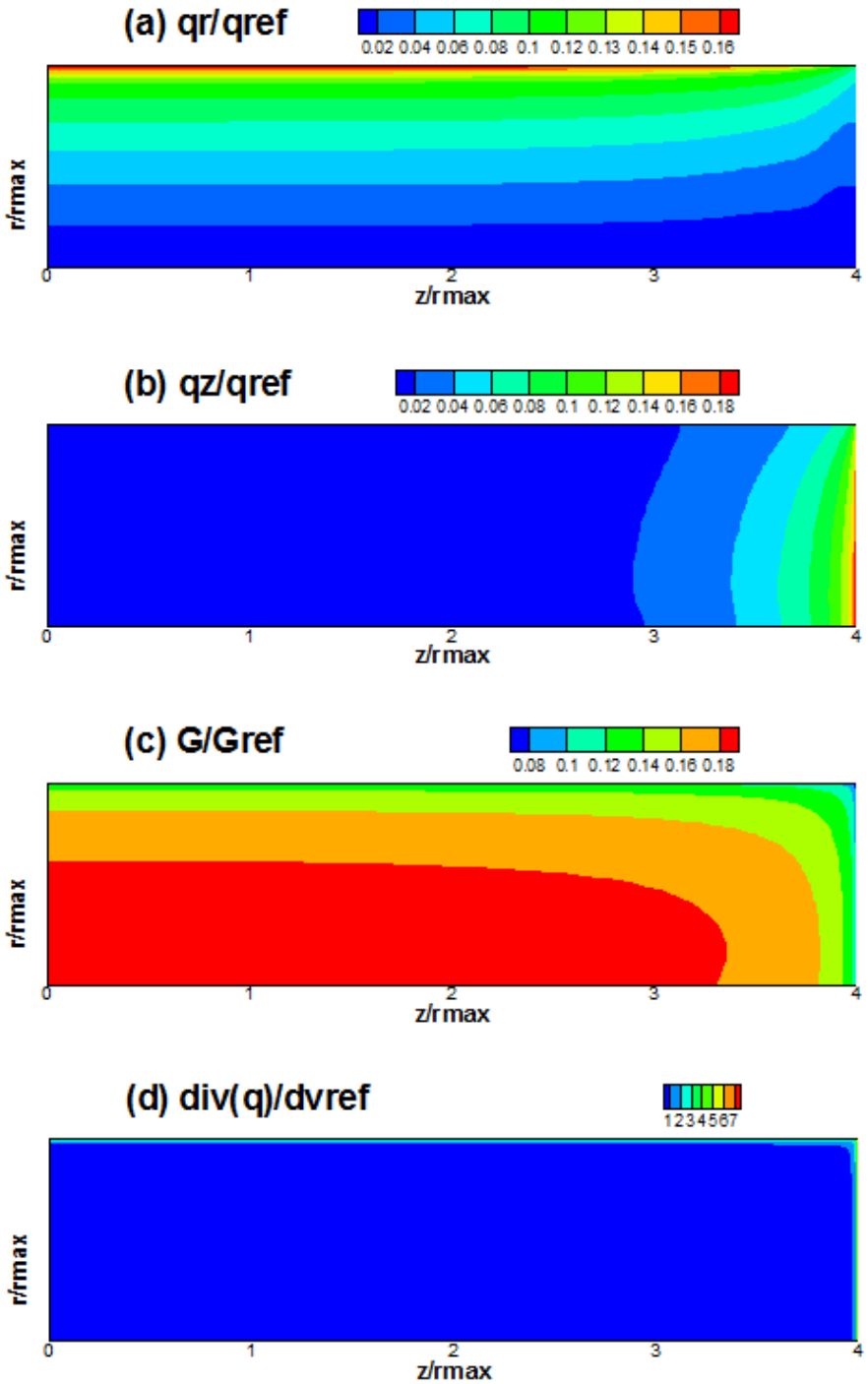

Figure 1.—Hot gas cylinder with cold walls: (a) radial heat flux, (b) axial heat flux, (c) mean radiant intensity and (d) heat flux divergence, optically thick case, $rmax = 1.0m$.

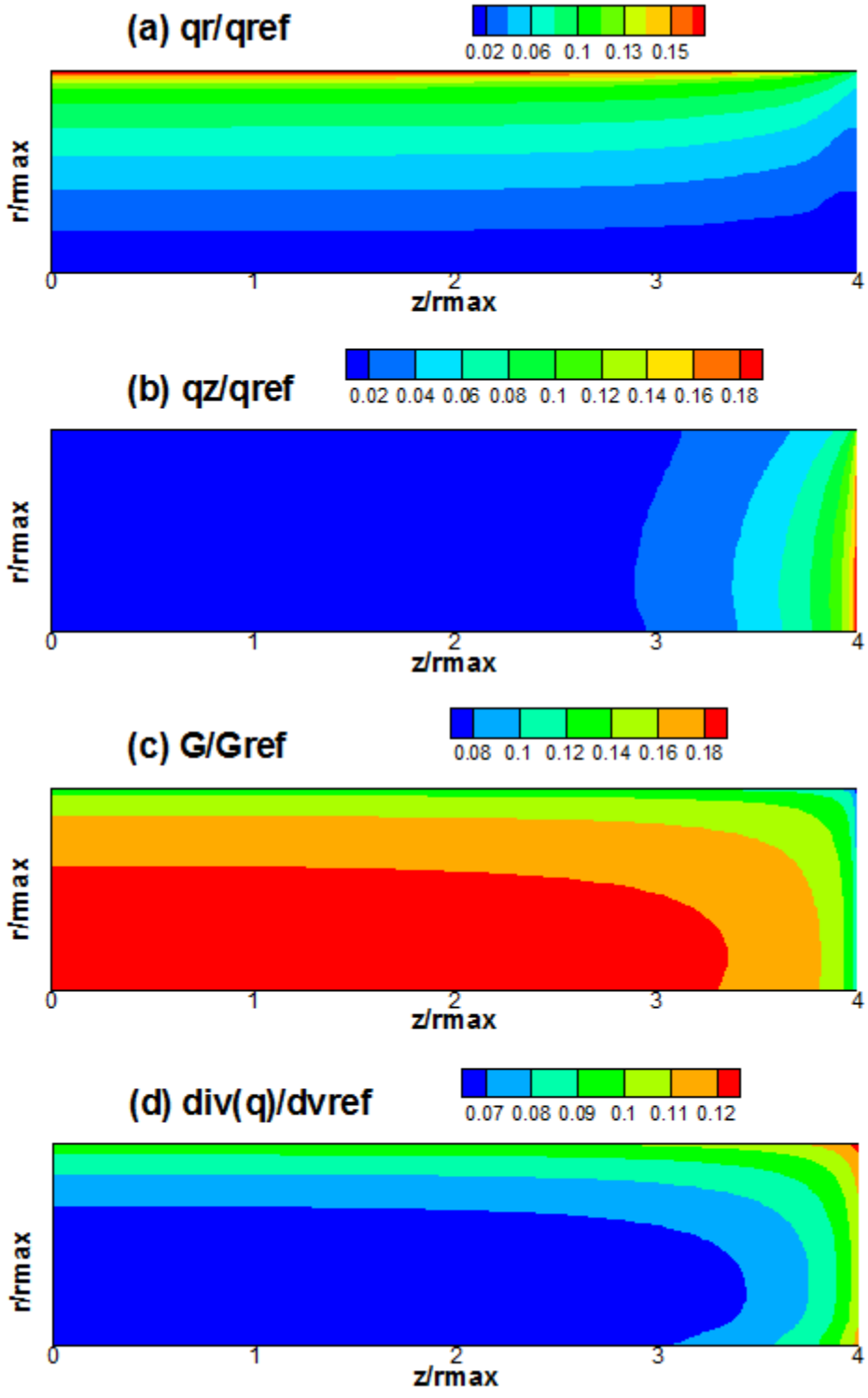

Figure 2.—Hot gas cylinder with cold walls: (a) radial heat flux, (b) axial heat flux, (c) mean radiant intensity and (d) heat flux divergence, optically thin case, $rmax = 0.01m$.

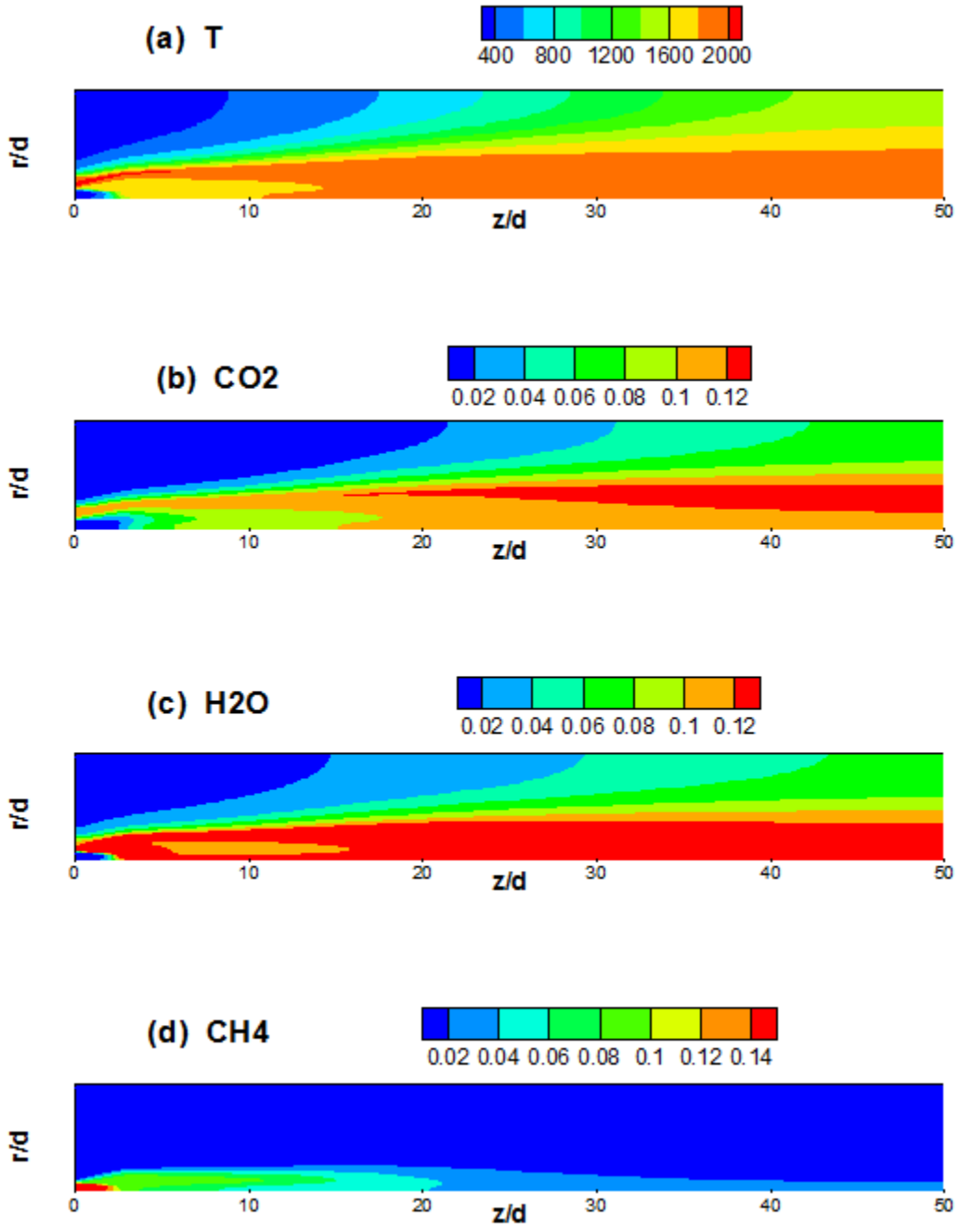

Figure 3.—Sandia Flame D—NCC results: (a) temperature distribution, (b) CO_2 mass fraction distribution, (c) H_2O mass fraction distribution, (d) CH_4 mass fraction distribution.

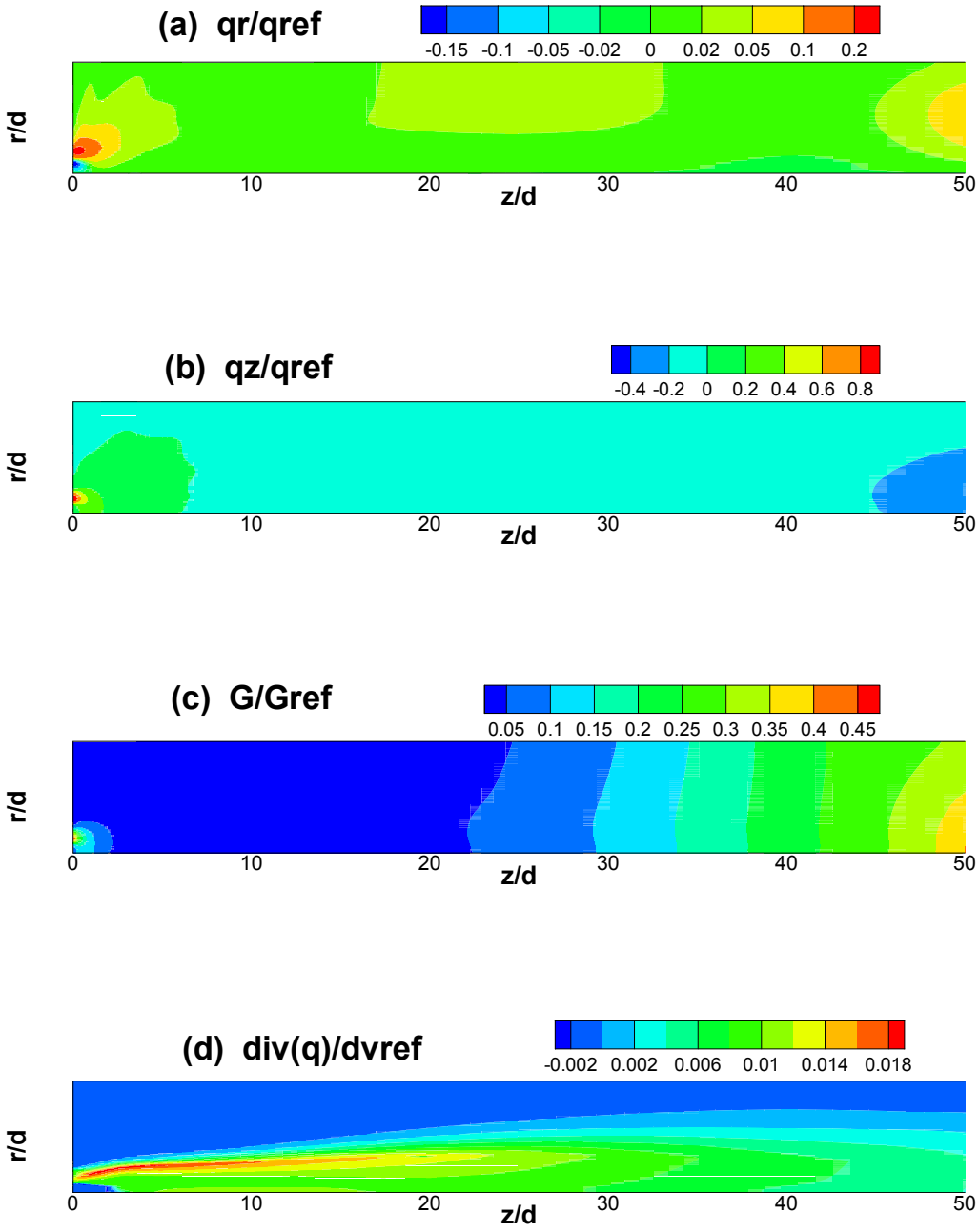

Figure 4.—Sandia Flame D—radiation results: (a) radial heat flux, (b) axial heat flux, (c) mean radiant intensity and (d) heat flux divergence.